

# Modular DAS Demodulation System Based on Ultra-Weak Fiber Bragg Gratings

LUO Zhihui; YANG Zhen; LU Bo; XU Bing; HUANG Jianglou

*College of Science, China Three Gorges University, Yichang 443002, China*

**Abstract:** To meet the requirements of low power consumption, miniaturization and massive data processing for DAS demodulation devices, this paper proposes a modular distributed acoustic sensing (DAS) demodulation system based on ultra-weak fiber Bragg gratings (UW-FBGs). A highly integrated embedded circuit is used for time-domain localization of gratings and data acquisition. The FPGA demodulates phase variations of each sensing segment in real time and uploads the demodulated results through a Gigabit Ethernet port. Tests on a PZT platform show that the system consumes less than 20 W, has dimensions of 250 mm x 180 mm x 45 mm, and the output data volume is approximately 2.6% of that of a conventional DAS system. The background noise from 5 Hz to 1280 Hz is 2.16  $\mu\text{e}/\sqrt{\text{Hz}}$  and the linearity is 0.9993. The system can work with an ordinary commercial notebook computer to acquire micro-vibration signals, providing a cost-effective solution for acoustic-level micro-vibration acquisition and field monitoring.

**Keywords:** distributed acoustic sensing; ultra-weak fiber Bragg grating; modularization; phase demodulation; embedded system

## Figure and Table Captions

Fig. 1 Operating principle of the DAS system.

Fig. 2 Arctangent demodulation flow based on a 3 x 3 coupler.

Fig. 3 Host software interface of the DAS system.

Fig. 4 Comparison of original and filtered signals.

Fig. 5 System test structure.

Fig. 6 Noise power spectral density of the DAS system.

Fig. 7 Time-domain and frequency-domain demodulated signals at 5 V and 5 Hz, 80 Hz and 1280 Hz.

Fig. 8 Voltage-phase curve.

Fig. 10 Comparison of music signal waveforms.

## 0. Introduction

Distributed acoustic sensing (DAS) is an emerging sensing technology capable of continuous distributed detection of vibration and sound fields. It offers large-area coverage, high resolution, high sensitivity and wide bandwidth, and has broad application prospects in pipeline monitoring, power cables and perimeter security. Conventional DAS is mainly based on phase-sensitive optical time-domain reflectometry (phi-OTDR), which measures micro-vibration by extracting the phase variation of Rayleigh backscattered light. Improving DAS performance has become an important research topic.

Although phase-noise compensation, multi-frequency methods and random fiber-laser amplification can improve sensitivity, Rayleigh scattering signals are weak and usually have poor signal-to-noise ratio and coherent fading. New designs improve performance but also increase algorithmic complexity and system cost. Enhancing scattering intensity by modifying the fiber provides a more economical way to achieve high SNR, and the use of ultra-weak fiber Bragg gratings with reflectivity around -40 dB to -50 dB and bandwidths generally above 3 nm at 3 dB has become attractive.

Compared with Rayleigh scattering, UW-FBG reflection improves signal strength by about 20 dB and SNR by nearly 30 dB, while also being compatible with draw-tower fabrication. However, many existing commercial or laboratory systems adopt X86 host-based demodulation, which requires large memory and real-time computation. A 250 MSPS DAS system may generate more than 1 GB/s of multi-channel phase data, resulting in high host volume and power consumption and reduced reliability in long-term operation.

To address these issues, a modular DAS system based on UW-FBGs is proposed. By introducing embedded circuitry for real-time processing of massive data, the system integrates configuration, acquisition and communication in a modular DAS host, reducing hardware requirements and power consumption while improving system performance.

## 1. Operating Principle of the DAS System

In the UW-FBG-based DAS demodulation system, continuous light emitted by a narrow-linewidth laser is modulated by a semiconductor optical amplifier (SOA), amplified by an erbium-doped fiber amplifier (EDFA), and coupled into the UW-FBG array. Reflected optical pulses from UW-FBGs at different locations reach the photodetector at different times, so each grating position can be identified by time-intensity analysis.

Reflected pulses from two adjacent gratings enter an unbalanced Michelson interferometer whose arm-length difference is equal to the spacing between adjacent gratings. The three outputs of a 3 x 3 coupler have phase differences of 120 degrees. After photoelectric conversion, three high-speed A/D channels acquire the signals synchronously. The embedded circuit completes arctangent phase demodulation, digital filtering and phase unwrapping in real time, and outputs the data via Ethernet. Faraday mirrors in the unbalanced Michelson interferometer compensate for polarization fading.

The embedded circuit is built around a Xilinx Zynq7035 device, which integrates an ARM processor and FPGA. It controls the timing of the SOA, EDFA and acquisition circuit and performs algorithm processing. Considering FPGA computing resources and grating-array scale, an arctangent phase demodulation algorithm based on trigonometric transformation is adopted. Phase unwrapping is introduced to remove arctangent phase discontinuities and achieve continuous demodulation over the full range.

## 2. Hardware Implementation and Signal Preprocessing

The modular DAS demodulation system integrates a narrow-linewidth light source, EDFA, unbalanced Michelson interferometer, detection circuits and embedded signal acquisition/processing board inside an aluminum-machined enclosure with external heat dissipation. It uses a 12 V DC power supply, has total power consumption below 20 W, and dimensions of 250 mm x 180 mm x 45 mm.

The embedded acquisition and processing board is the core of the system. It includes the Zynq7035 processor and peripherals, optical pulse modulation, A/D acquisition and interface circuits. Analog signals from the three photodetectors are converted to differential signals through AD4930 devices, and two high-speed A/D chips complete three-channel digitization at 250 MSPS with 14-bit resolution. A single digital channel produces about 500 MByte/s of data. The FPGA reads the conversion results at about 1.5 GByte/s, filters data according to grating positions, calculates the phase of each sensing segment and sends the results to the host computer.

With UW-FBGs spaced at 5 m as sensing units, a 2.5 km fiber contains 500 sensing segments. At a sampling frequency of 33 kHz, each sensing-unit phase value is represented by 2 bytes. Including Ethernet protocol overhead, the real-time transmission rate is about 40 MByte/s, only about 2.6% of the data volume of conventional demodulation, greatly reducing host-computer processing load.

To display phase data from each sensing unit in real time, a C# user interface was developed. It includes user settings, a waterfall plot, time-domain plot and spectrum plot. The waterfall plot shows the position and intensity of vibration events and their temporal evolution. The time-domain and frequency-domain plots show the phase variation and spectral distribution of a selected sensing unit. System parameters such as pulse width, sampling frequency, EDFA current, filter type and data storage path can be configured. An initialization interface is also provided for personalized parameter settings and grating-position storage.

Original phase signals usually contain multiple components. A digital preprocessing interface is included in the host software for secondary development according to user needs. For example, a Butterworth digital filter is used to remove low-frequency interference. Since digital filters have requirements on data-flow length, abrupt changes may occur at the beginning and at frame boundaries; therefore, extended data streams and smoothing are applied to improve filtering and ensure frame continuity.

## 3. Performance Testing and Analysis

A test platform was built to verify the performance of the UW-FBG DAS system. The modular DAS demodulator had a center wavelength of 1550.12 nm. The sensing array had 5 m grating spacing, reflectivity of -40 dB, bandwidth of 5 nm at 3 dB and length of 60 m. A piezoelectric ceramic (PZT) actuator with an inner diameter of 80 mm and radial coefficient of 0.125  $\mu\text{m}/\text{V}$  was used as the strain loading device. The demodulator sampling period could be selected between 30  $\mu\text{s}$  and 100  $\mu\text{s}$ , and pulse width was set to 32 ns.

Approximately 1 m of grating fiber between the sixth and seventh grating points was wound on the PZT. The UW-FBG array was connected to the DAS demodulation module. A computer-controlled signal generator applied sinusoidal signals of different frequencies and voltages to the PZT to simulate vibration, while a commercial notebook computer displayed the demodulation results. Background noise and response characteristics were mainly evaluated.

### 3.1 Background Noise

In a quiet laboratory environment with no external sound-field excitation, the fourth grating sensing unit in the middle of the array was selected to avoid interference from false signals at the fiber head or tail. The measured phase noise was approximately 0.01 rad, and the noise power spectral density was about -80 dB rad/ $\sqrt{\text{Hz}}$ . The corresponding system background noise was calculated to be 2.16 p $\epsilon$ / $\sqrt{\text{Hz}}$ .

### 3.2 Response Characteristics

To evaluate sensitivity and frequency response, the signal generator produced a 5 V excitation signal at 5 Hz, 80 Hz and 1280 Hz. Different sampling frequencies were used for phase output. The DAS system recorded sinusoidal waveforms and spectra with high fidelity. When the sampling period is 30  $\mu\text{s}$ , the Nyquist theorem indicates that the system can theoretically acquire signals up to 16.5 kHz without distortion. Because the fiber and PZT were not permanently bonded, slight waveform distortion occurred at the top of the sine wave when the voltage bias was high.

With the excitation frequency fixed at 200 Hz, the voltage was increased from 1 V to 10 V in steps of 1 V. Linear fitting of the output phase showed that the demodulated phase increased linearly with driving voltage. The linearity was 0.9993 and the slope was 1.943 rad/V.

### 3.3 Music Playback Test

To evaluate overall system performance, music signals were acquired using DAS. The speaker of one mobile phone served as the sound source. A bare-fiber sensing unit was wound into a ring with a diameter of 10 cm, suspended facing the speaker at a distance of 30 cm, and another mobile phone was placed below the fiber ring for synchronous recording. The time-domain signals demodulated by DAS, the original music signal and the mobile-phone recording had generally consistent normalized trends. The amplitude of the DAS signal was slightly lower than the original sound but followed the fluctuations closely, while the mobile-phone recording showed many spikes and severe amplitude distortion. The DAS recording fidelity was obviously better than that of the commercial phone. When the demodulated waveform was packaged as an audio file at the demodulation sampling rate, it could be played back clearly, demonstrating that the DAS system can effectively capture sound-field signals.

## 4. Conclusion

This paper proposes and validates a modular DAS demodulation system based on UW-FBGs. Embedded circuitry completes 3 x 3 arctangent phase demodulation and solves the problem of massive data communication and processing, reducing uploaded data to about 2.6% of conventional DAS. Integrated optical modulation, control, signal processing and communication reduce the system volume to 250 mm x 180 mm x 45 mm and power consumption to less than 20 W. The theoretical maximum detection frequency is 16.5 kHz, the background noise is 2.16 p $\epsilon$ / $\sqrt{\text{Hz}}$  and the linearity is 0.9993. With its small size, low power consumption, high sensitivity and flexible signal-processing interface, the system provides a friendly platform for secondary development and has good application prospects.

## References

*Reference entries are retained in the original citation form to avoid altering source bibliographic data.*

苑立波,童维军,江山,杨远洪,孟洲,董永康,云江,何祖源,靳伟,刘统玉,邹琪琳,毕卫红.我国光纤传感技术发展路线图[J].光学学报,2022,42(01):9-42.

孙琪真,范存政,李豪,闫宝强,闫志君,余刚,刘德明.光纤分布式声波传感技术在石油行业的研究进展[J].石油物探,2022,61(01):50-59+77.

桂鑫,李政颖,王洪海,王立新,郭会勇.基于大规模光栅阵列光纤的分布式传感技术及应用综述[J].应用科学学报,2021,39(05):747-776.

Wu Mengshi,Fan Xinyu,Liu Qingwen,He Zuyuan. Highly sensitive quasi-distributed fiber-optic acoustic sensing system by interrogating a weak reflector array.[J]. Optics letters,2018,43(15).

冉曾令,饶云江,王熙明,肖彦波,余刚,安树杰,陈沅忠,吴俊军.uDAS-?分布式光纤传感地震仪及其应用[J].石油物探,2022,61(01):41-49.

Yi Xin Zhang,Si Yi Fu,Yu Sheng Chen,Zhe Wen Ding,Yuan Yuan Shan,Feng Wang,Meng Meng Chen,Xu Ping Zhang,Zhen Meng. A visibility enhanced broadband phase-sensitive OTDR based on the UWFBG array and frequency-division-multiplexing[J]. Optical Fiber Technology,2019,53(C).

黄俊斌,丁朋,唐劲松.弱反射光纤光栅阵列制备、解调与应用进展[J].激光与光电子学进展,2021,58(17):62-79.

唐健冠,刘宇哲,李成立,郭会勇,杨明红.基于超弱光纤布拉格光栅的高信噪比分布式振动传感系统[J].光学学报,2021,41(13):118-124.

王晨,吕公河,徐雷良,牟风明,尚盈.基于弱光栅阵列相位载波解调的分布式井中地震勘探技术研究[J].石油物探,2022,61(01):78-84.

Li Chengli,Tang Jianguan,Jiang Yanshi,Cheng Cheng,Cai Longbao,Yang Minghong. An Enhanced Distributed Acoustic Sensor With Large Temperature Tolerance Based on Ultra-Weak Fiber Bragg Grating Array[J]. IEEE PHOTONICS JOURNAL,2020,12(4).

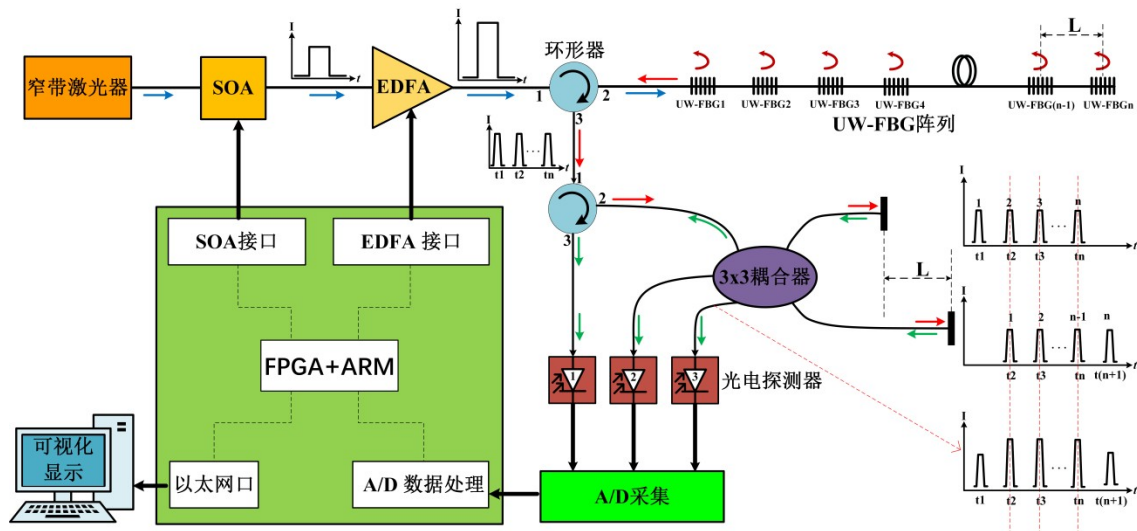
刘德明,贺韬,许志杰,孙琪真.新型微结构光纤分布式声波传感技术及应用[J].应用科学学报,2020,38(02):296-309.

David Atubga,Huijuan Wu,Lidong Lu,Xiaoyan Sun. Comparative study of lossy and lossless data compression in distributed optical fiber sensing systems[J]. Optical Engineering,2017,56(2).

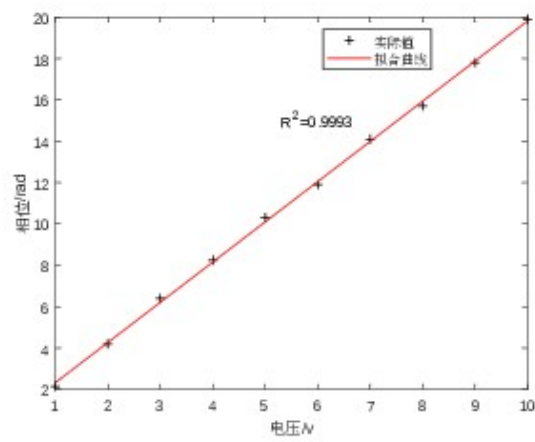
## Retained Figures and Visual Materials

The original figures, screenshots, diagrams and experimental plots from the source manuscript are retained below in their original order for layout continuity. Captions in the translated body follow the the source numbering where available.

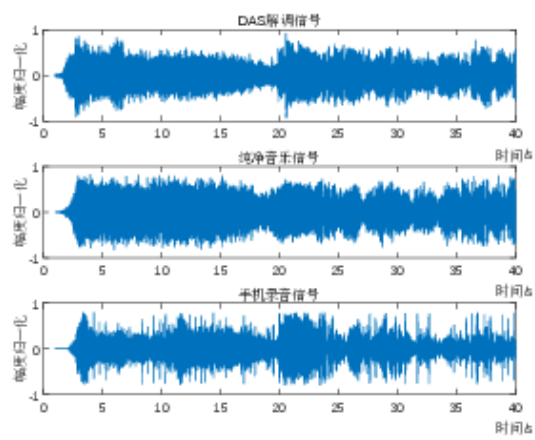
Original visual material 1



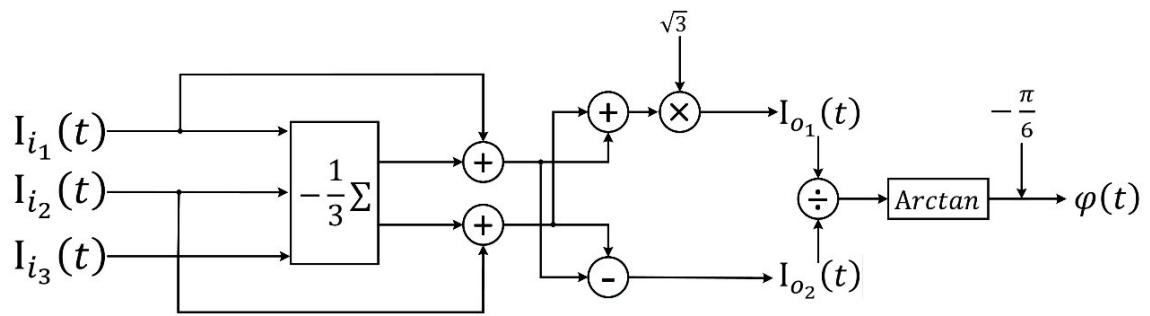
Original visual material 2



### Original visual material 3



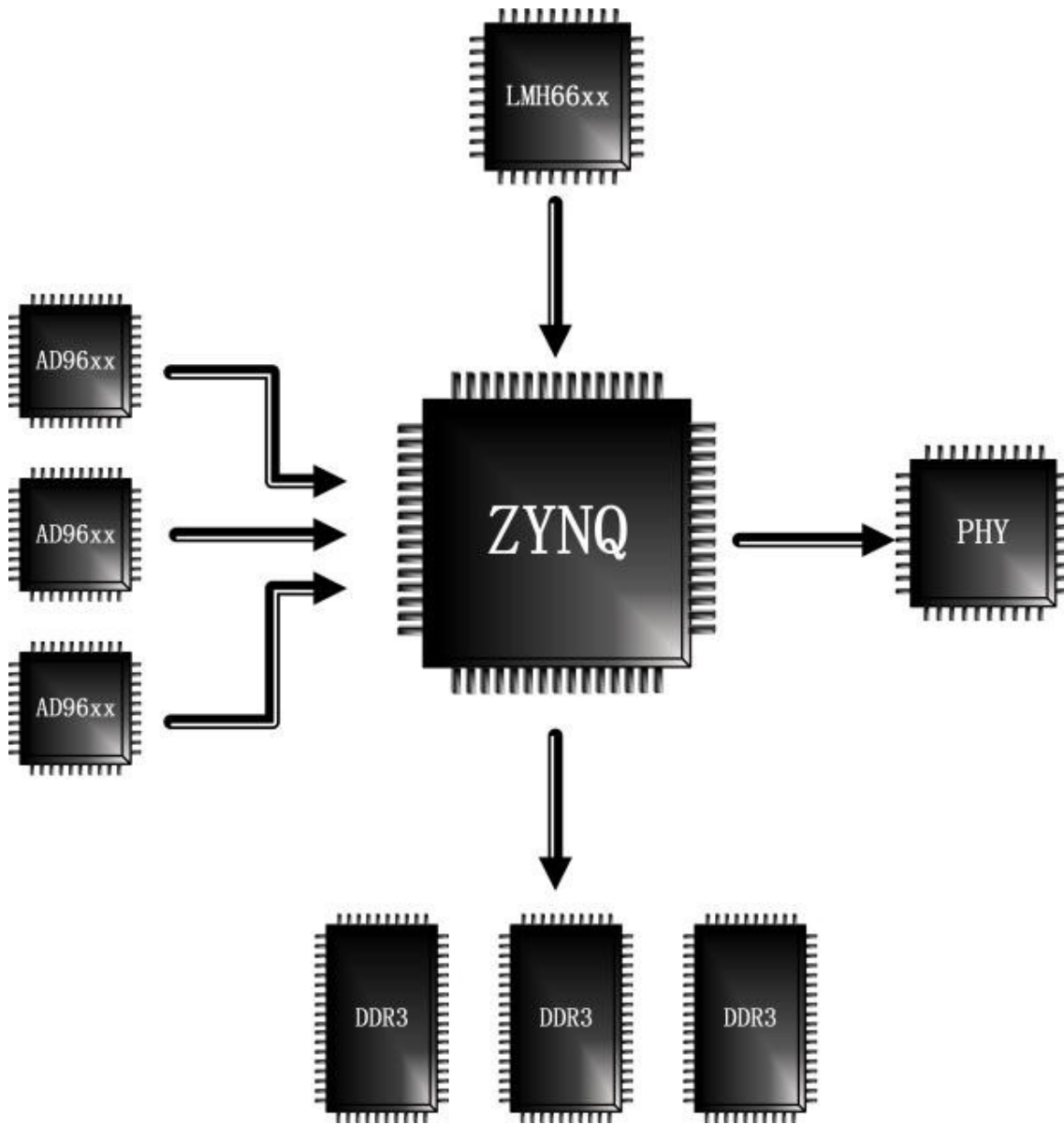
#### Original visual material 4



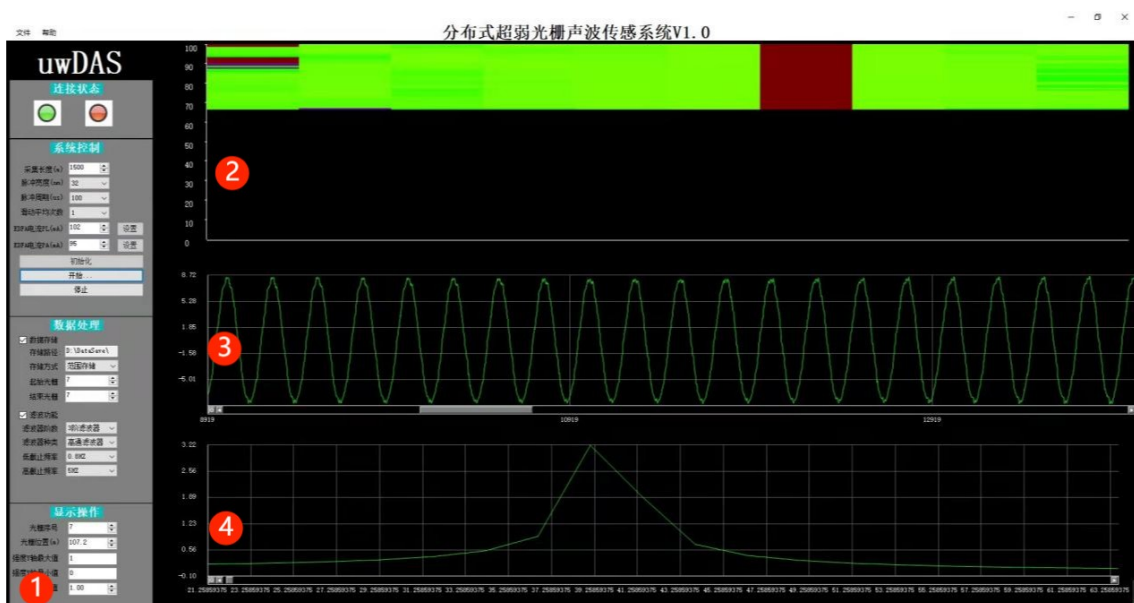
Original visual material 5



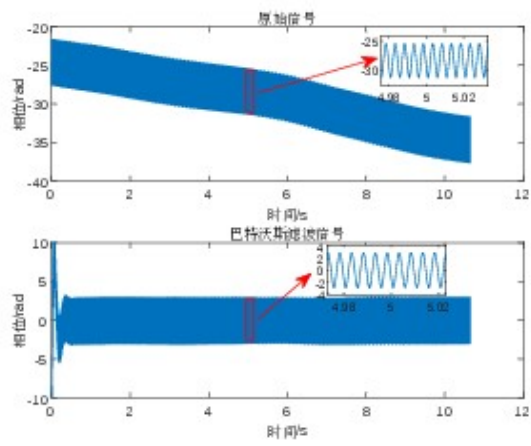
Original visual material 6



Original visual material 7



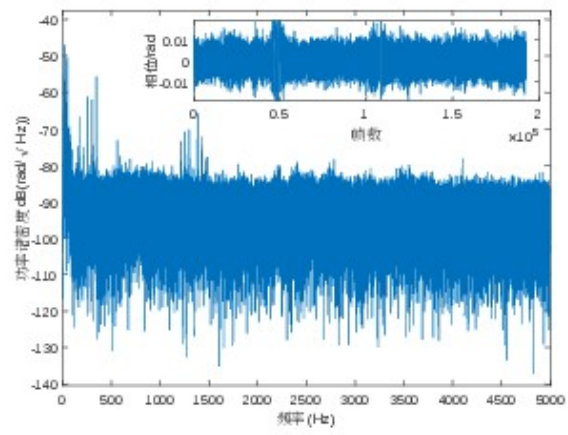
Original visual material 8



Original visual material 9



Original visual material 10



Original visual material 11

